AIAA JOURNAL
Vol. 39, No. 5, May 2001

Mesoscale Structural Characterization Within Bulk Materials by High-Energy X-Ray Microdiffraction

U. Lienert*
European Synchrotron Radiation Facility, F-38043 Grenoble CEDEX, France
H. F. Poulsen†
Risø National Laboratory, DK-4000 Roskilde, Denmark
and
Å. Kvick‡
European Synchrotron Radiation Facility, F-38043 Grenoble CEDEX, France

A novel diffraction technique for the local three-dimensional characterization within polycrystalline bulk materials is presented. The technique uses high-energy synchrotron radiation (40 keV < E < 100 keV), which penetrates deeply into materials. Focusing broadband optics have been developed that provide the required intensity and spatial resolution perpendicular to the incident beam. A focus size of 1.2 μm was achieved. Modified crossed-beam techniques are being developed that define the longitudinal resolution, i.e., the component of the gauge volume parallel to the incident beam. We present experimental evidence that a longitudinal resolution down to 10 μm can be obtained. Fundamental materials properties such as the strain/stress state, grain-orientation, -size, and -surface topology can be probed and mapped in three dimensions in favorable cases. Imbedded volumes and interfaces become accessible. The technique is nondestructive and allows for in situ studies of samples in complicated environments. A dedicated experimental station has been constructed at the ID11 beamline of the European Synchrotron Radiation Facility. On-line two-dimensional detectors and conical slits have been developed. Four examples of applications are presented.

I. Introduction

DIFFRACTION techniques play a central role in the structural characterization of polycrystalline materials. It is important to probe bulk properties for a wide class of systems where the macroscopic parameters are not represented by the particular properties close to surfaces. In most cases the macroscopic properties like texture, flow stress, fatigue strength, corrosion resistance, magnetization, or superconducting critical current will depend on the microstructural parameters within the bulk such as the local strain/stress state, dislocation density, grain-size, -orientation, or grain-boundary topology. Two well-established diffraction techniques are electron microscopy and neutron diffraction. Electron microscopy provides a spatial resolution down to atomic distances, but the electrons cannot penetrate into the bulk because of their strong interaction with matter. Neutrons, on the other hand, can penetrate some centimeters into many materials, but the spatial resolution is only on the millimeter scale.[1] The technique presented here uses high-energy synchrotron radiation (40 keV < E < 100 keV), which can penetrate sufficiently deeply into materials (see Fig. 1) and allows, at the same time, for a spatial resolution on the micrometer scale. The technique is nondestructive and fills the wide gap between electron and neutron diffraction methods. The large penetration power of high-energy x rays also allows for in situ studies with a complicated sample environment, i.e., thermomechanical processing.

Dedicated beamlines for high-energy x-ray diffraction have become available at several synchrotrons. Although small beams are most easily produced by inserting apertures, this method is limited by the decreasing ratio of transmitted flux to edge scatter as the aperture size decreases; apertures cannot provide useful beams smaller than ~10 μm. However, as outlined later, microfocusing broadband optics allows the production of intense beams with a spot size down to ~1 μm. Microfocusing requires a sufficiently narrow source size, which is only provided by third-generation synchrotrons, such as the European Synchrotron Radiation Facility (ESRF) in Grenoble, France. A first dedicated experimental station utilizing high-energy, focusing broadband optics has been constructed at the ESRF Materials Science Beamline (ID11). The project,[2] referred to as three-dimensional x-ray diffraction (3DXRD), is a collaboration with the Materials Research Department of the Risø National Laboratory in Denmark and aims to achieve a spatial resolution of $5 \times 5 \times 50$ μm^3 as a routine point probe. As described next, the resolution might be further improved in selected dimensions if only a line focus is required and by focusing analyzer optics.

The paper is organized as follows: First, some basic principles are outlined that are of fundamental importance for the 3DXRD technique. Second, the instrumentational developments that are required by the novel technique are described. Finally, four case studies are presented to illustrate the scope of the technique. The examples are feasibility studies from the development phase of the project and were performed at the ESRF beamlines BM5, ID11, and ID15. Further applications, including in situ studies, are published elsewhere.[3,4]

II. Basic Principles

A. Penetration Depth

The samples are generally investigated in transmission geometry as a result of the small Bragg angles within the energy range of interest 40–100 keV. Typically, a transmission down to 10% still provides sufficient flux and signal-to-noise ratio. The absorption of x rays in matter is described by a linear attenuation coefficient. For light elements inelastic (Compton) scattering is the dominant absorption process, whereas photoelectric absorption dominates for elements of medium or high atomic number Z. The inelastic attenuation coefficient varies only slowly with energy, whereas the photoelectric attenuation coefficient scales in absence of absorption edges roughly with E^{-3} and $Z^{4.5}$. The attenuation coefficient increases by about a factor of five at K-absorption edges. Sample thicknesses that relate to 10% transmission are plotted in Fig. 1 for selected elements and energies.

Received 23 September 1999; revision received 20 June 2000; accepted for publication 7 July 2000.

*Beamline Scientist, Experiments Division; currently Staff Physicist, Advanced Photon Source X-Ray Physics Group, Argonne National Laboratory, 9700 South Cass Avenue, Argonne, IL 60439.
†Senior Scientist, Materials Research Department.
‡Senior Scientist, Experiments Division.

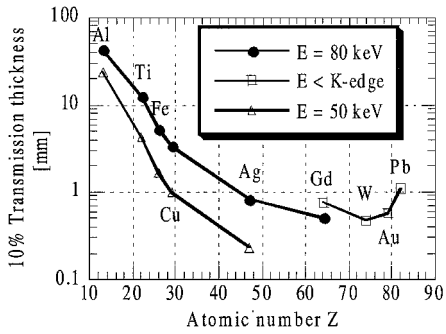

Fig. 1 Penetration depth of high-energy x rays for selected elements. Values are given for energies of 50 and 80 keV up to medium Z and just below the K absorption edges for large Z elements.

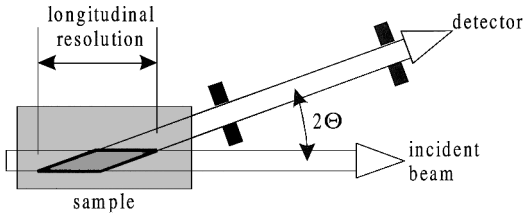

Fig. 2 Sketch of the crossed-beam technique to define the longitudinal resolution.

B. Source Imaging

Focusing optics provides the spatial resolution perpendicular to the incident x-ray beam, referred to as transversal resolution. A fundamental limitation of the achievable focus size is set by the source size times the demagnification factor, i.e., the ratio of the optics-to-focus and source-to-optics distances. A compromise must be found as a short optics-to-focus distance, called focal length, provides higher source demagnification but also increases the convergence and therefore degrades the Q-space resolution. Furthermore, a focal length of the order of 1 m is required to allow for bulky samples and environments. Therefore, a narrow source size is required by microfocussing of high-energy x rays for diffraction applications.

C. Bandwidth Allowance

Experiments at high energies and narrow spatial resolution are notoriously flux limited. Broadband monochromators are therefore used to increase the flux preventing long data acquisition times. We have chosen the upper limitation of the bandwidth so as to detect lattice strain variations of $\Delta d/d$ larger than 10^{-4}. According to Braggs law

$$2d \sin(\Theta) = \lambda \tag{1}$$

changes in the lattice spacing d can be detected as shifts of the 2Θ position of the center of the corresponding diffraction peak. Assuming that the peak center can be determined to 1% of the peak width and for a typical scattering angle of $2\Theta = 6$ deg, the tolerable beam convergence and energy bandwidth are obtained from the differential form of Eq. (1) as $\Delta\Phi = 1$ mrad and $\Delta E/E = 1\%$. Compared to a standard, nonfocusing perfect crystal monochromator, the energy bandwidth and horizontal and vertical convergences can therefore be increased by a factor of 100. Hence, the intensity can be increased by about six orders of magnitude as compared to standard, nonfocusing perfect crystal monochromator optics.

D. Crossed-Beam Technique

The spatial resolution parallel to the incident beam, referred to as longitudinal resolution, is obtained by the crossed-beam technique. The setup is sketched in Fig. 2. A narrow (focused) beam traverses the sample. The transversal positions of the diffracted beams are confined by slits at two distances behind the sample. The intersection of the incident beam and the selected diffracted beams spans the gauge volume. Ideally, the first slit should be as close to the gauge volume as possible. However, the gauge volume will always be elongated in the direction of the incident beam as a result of the small scattering angles. Assuming that the transversal beam position can be confined to 5 μm and for a scattering angle of $2\Theta = 6$ deg, the projection along the incident beam amounts to 50 μm.

In some situations a degradation of the total resolution by the large longitudinal component can be avoided by aligning the sample in a suitable direction with respect to the incoming beam or, if grain boundaries are being mapped, by scanning the sample in the direction of the beam and defining the grain boundary as being positioned at the half intensity point. Various systematic errors can arise for local strain mappings depending on the actual geometry (see e.g., Refs. 5 and 6). However, a detailed discussion of these errors and their treatment is beyond the scope of this paper.

III. Instrumentation

A. Experimental Station

The 3DXRD experimental station is accommodated in an extension hutch to the existing ID11 beamline. It is 10 m long and centered at 56 m from the radiation source point of the storage ring. The Pb hutch provides sufficient radiation protection that 1 mm^2 of direct beam can be taken into the hutch. Experiments are remotely controlled from the adjacent control hutch.

The synchrotron radiation is produced by a wiggler or a recently installed in-vacuum undulator. The source size (full width at half maximum) is about 30 μm in the vertical and 150 μm in the horizontal direction. The source limited focus size is about 1 μm vertically and 5 μm horizontally for a typical demagnification factor of 30.

The focusing optics are accommodated in a Pb tank at the beginning of the hutch. The Pb tank provides a local scattering shielding reducing the background seen by the detectors.

The horizontal diffractometer provides two axes of rotation. The sample stage supports a load of up to 200 kg. Particular care was taken by the selection of the sample ω rotation table. A concentricity better than 0.5 μm is required to maintain the active sample volume during sample rotations. The main design goal of the diffractometer was to ensure the necessary stability for strain measurements. Therefore, advantage was taken from the fact that scattering angles are small at high x-ray energies. The detector (2Θ) arm is constructed as a 3-m-long granite bench that pivots around the sample axis. The bench is driven by a linear translation stage that moves perpendicular to the incident beam. The angular range of the detector arm is restricted from about -4 to $+18$ deg. Detectors can be mounted on two platforms that can be translated along the bench.

There is 5 m of free space behind the diffractometer to either improve the Q-space resolution by an increased sample detector distance or to accommodate additional equipment.

B. Focusing Monochromators

At classical x-ray energies (5–30 keV) various techniques have been developed to achieve microfocusing of synchrotron radiation. However, we consider that bent Laue crystals and multilayers are the most promising focusing elements at high energies.

1. Multilayers

Periodic multilayers are stacks of alternating layers of high- and low-electron density materials, which are grown on highly polished substrates. At each interface a fraction of the incident intensity is specularly reflected, and reflectivities up to 80% are obtained when the Bragg condition is fulfilled. The bandwidth of periodic multilayers is around $\Delta E/E = 1\%$, fully exploiting the bandwidth allowance and providing maximum flux.[7] Multilayers must be operated in reflection geometry, and we require 30-cm-long substrates to cover 1 mm of incident beam height. Shorter substrates could be used by decreasing the layer thicknesses and therefore increasing the Bragg angle, but this is limited by the increasing fraction of the diffuse scattering. Focusing is obtained by bending the substrates to elliptical shape (Fig. 3) so that the source and focus points must coincide with the focal points of the ellipse. In elliptical geometry the incidence angle of the x-ray beam changes along the footprint, and hence the layer thicknesses are correspondingly adapted to prevent a further increase of the bandwidth. The actual focal spot size is limited by the imperfect surface finish of the substrates.

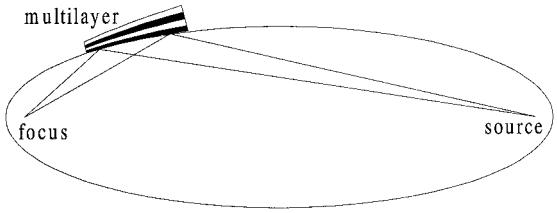

Fig. 3 One-dimensional focusing by a bent, graded multilayer in elliptical geometry.

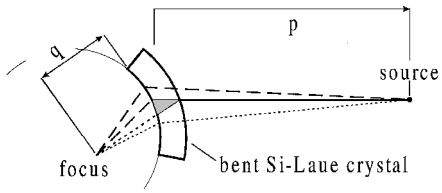

Fig. 4 Microfocusing by a bent Laue crystal. The rays indicated by long/short dashes represent low/high energies.

2. Bent Laue Crystals

The standard monochromator scheme for synchrotron radiation uses low-order reflections from perfect Si crystals providing a narrow bandwidth of about $\Delta E/E = 10^{-4}$. Focusing is achieved by bending the Si crystal. The bending also perturbs the perfect crystal periodicity, and hence the x rays are diffracted from a larger crystal volume, and the bandwidth increases. Unfortunately, this volume effect limits in general the achievable focus size. The focus broadening can be overcome only in Laue (transmission) geometry by choice of a particular asymmetric cut[8] (Fig. 4); the bandwidth of the actual bent Laue monochromators is $\Delta E/E = 5 \times 10^{-4}$.

Contrary to the multilayer, the incoming beam impinges almost perpendicular onto the crystal, and the footprint on the crystal is short. The normal incidence results in substantial technical advantages. However, the lattice plane spacing of the perfect crystal cannot be tailored along the footprint of the incident beam, and the total bandwidth depends therefore on the size of the incident beam. For 1 mm of incident beam, the total bandwidth amounts to $\Delta E/E = 0.6\%$, but the Q-space resolution can be improved by accepting less beam.

3. Point Focusing

A single bent multilayer or Laue crystal provides only focusing in one dimension, i.e., a line focus. Point focusing is achieved by combination of either two multilayers[9] or a Laue crystal and a multilayer, the scattering planes of the combined elements being perpendicular.

C. Status of Optics Performance

Experiments have been performed between 50 and 90 keV. The optical elements were found to be stable under the heat load of the incident beam, and a good signal-to-background ratio was obtained. A 3.6-μm-wide line focus was obtained with the bent Laue crystal, and point focusing was achieved down to $4 \times 6\ \mu m^2$. The measured photon flux agrees with the expectations; about 10^{11} and 10^{12} ph/s were measured behind the Laue crystal and multilayer, respectively.

D. Detectors

A two-dimensional, high-resolution position sensitive detector is under development in which a spatial resolution of 5 μm should be achieved. The good spatial resolution is required for experimental settings that allow fast data acquisition by defining the local gauge volume directly by the detector resolution. The detector consists of a fluorescence screen that converts the x rays into visible light, a coupling lens optics, and a charge-coupling device (CCD) detector. The spatial resolution depends mainly on the thickness of the fluorescence screen, thinner screens giving better resolution. On the other hand, the absorption becomes small for thin screens and the detector inefficient. Scintillators are therefore required that contain high Z elements to increase the absorption. The detector is semitransparent to the incoming x rays, i.e., the transversal position of the beams can also be measured behind the detector. It is important to position the detector close to the sample to define narrow gauge volumes. First tests of the detector revealed a resolution of 15 μm. The reasons for the discrepancy from the expected resolution are under investigation.

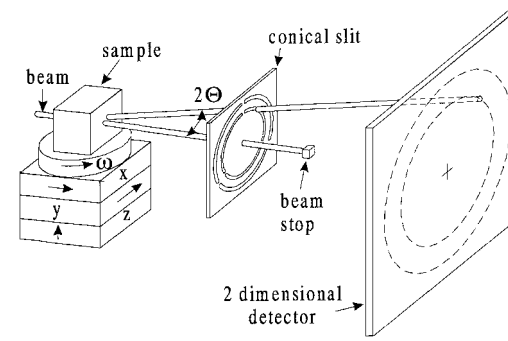

Fig. 5 Setup of a conical slit cell to map grain boundaries.

Another CCD detector (XIOS-II) that is coupled by a fiberoptical taper to a fluorescence screen provides a resolution of 80 μm. The camera is generally placed far behind the sample and measures the scattering angles.

E. Definition of the Longitudinal Resolution

The basic crossed-beam technique as just outlined has some practical drawbacks. First, a precise and tedious crystallographic alignment of the sample is required if the gauge volume does not contain a sufficient number of randomly oriented grains. Second, three-dimensional mappings will be time consuming as only one volume element can be probed at a time. Third, the transversal position must be measured as close to the gauge volume as possible to achieve good spatial resolution; this may conflict with the size of the sample or sample environment. Also, aperture openings below 5 μm seem not to be feasible, which limits the longitudinal resolution to about 50 μm. Therefore, the following modified crossed-beam techniques are being developed.

A (second generation) conical slit cell was manufactured by spark cutting.[10] The conical geometry allows us, in combination with a position sensitive detector, to observe simultaneously the full Debye–Scherrer cones of the investigated reflections. The principle setup as used in the copper grain mapping experiment described next is sketched in Fig. 5. The width of the conical slit openings is 25 μm. The slit cell contains six concentric conical slit openings, which select low-order reflections from samples with a face-centered cubic structure. By evaluation of the diffraction rings, a texture analysis can be performed without rotating the sample.

In some cases the illuminated sample volume does not contain a large enough number of grains such that distinct reflections still arise rather than continuous diffraction rings (the study of prestrained steel samples described next falls into this category). In this case the conical slit cell might be replaced by the semitransparent, high-resolution position sensitive detector just described. The positions and orientations of the grains may then be tracked back from the transversal positions of the reflections observed on the two position sensitive detectors. The same principle is employed in high-energy physics using three-dimensional detectors. It is sufficient to focus the incident beam in one dimension, and a complete layer can be mapped simultaneously. A detailed description of the technique is given in Ref. 11.

As just mentioned, elliptically shaped multilayers provide one-dimensional imaging. Another multilayer can be arranged behind the sample such that a magnified image is produced of the diffracted intensity along the beam trajectory in the sample (Fig. 6). The longitudinal resolution is obtained either by observing the image on a position sensitive detector or by selecting some fraction of it by a slit. It is then possible to apply the standard crossed-beam technique, but now the first slit can be effectively placed infinitesimally close to the magnified image. Furthermore, the longitudinal resolution does not depend directly on the distance between sample and multilayer, and bulky sample environments can be used. The focusing analyzer

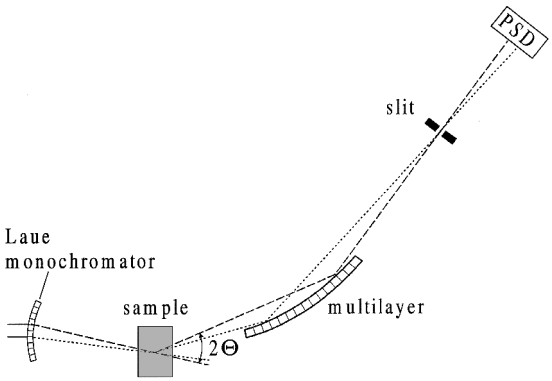

Fig. 6 Definition of the longitudinal resolution by a focusing multilayer analyzer. (For description see text.)

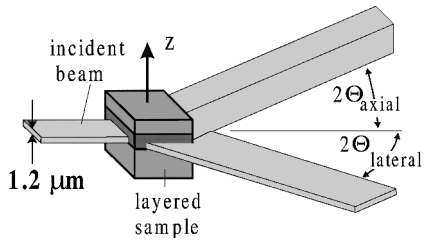

Fig. 7 Scattering geometry of the strain gradient mapping of layered structures. The samples are scanned in z direction, and the axial and lateral diffraction angles are recorded simultaneously.

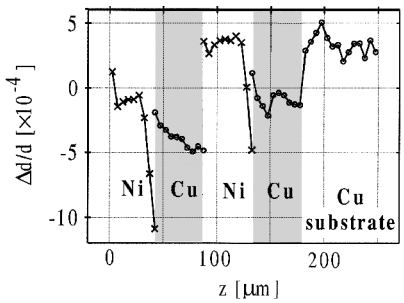

Fig. 8 Residual strain gradients in a structural Cu/Ni multilayer as function of depth below the surface z. Plotted are the relative d-spacings of the axial [2 0 0] reflection. The structure consists of two 90-μm-thick electrodeposited Ni/Cu bilayers on a Cu substrate. The samples were about 2.5 mm thick. Note the steep gradients at the buried Ni-Cu interfaces.

scheme was realized experimentally, and an achievable longitudinal resolution of 10 μm was inferred.[12]

IV. Case Studies

A. Strain Gradients in Layered Structures

The depth-dependent strain gradient in layered Cu/Ni structures was measured.[7] The penetration power of the high-energy x rays allows us to employ transmission geometry (Fig. 7). A bent Laue crystal focussed 90-keV x rays to an 1.2-μm-wide line. The samples were scanned perpendicular to the beam obtaining a depth resolution of the same size as the focus width. The longitudinal resolution was not confined, but the signal was averaged along the full sample thickness where the surface regions contribute only a small amount. In this way strain gradients across the buried Cu/Ni interfaces were measured, which is not possible by other techniques. The actual strain gradient was recorded by measuring the position of the diffracted beams far away from the sample. Steep strain (and texture) gradients were observed at the Cu/Ni interfaces (Fig. 8). The strain gradients are suggested to be caused by recrystallization processes during the electrodeposition. Further applications of macrostrain scanning are given in Refs. 13 and 14.

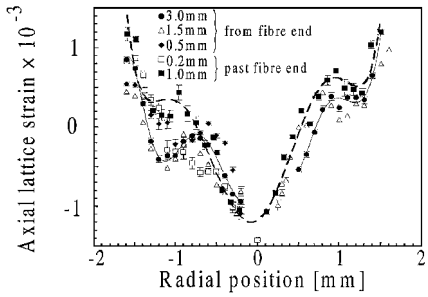

Fig. 9 [111] axial lattice strain as a function of radial position at several axial positions in a Cu sample with a 4.5-mm-long, 0.5-mm-diam W-fiber along the axis: ——, polynomial fit to the closed circles; and – – –, fit to the closed squares.

B. Local Strain Contours Around Inclusions in Wire-Drawn Cu/W Composites

The aim of this experiment was to investigate the local strain field around embedded inclusions in composite samples.[15] Composite samples were produced by casting copper around a continuous, single-fiber W inclusion of 0.5 mm diam. The samples were wire drawn and recrystallized in several steps, reducing the initial sample diameter from 8 to 3.2 mm. The average grain size in the Cu matrix was such reduced to 5 μm, and the axial W fibers were broken up into short, spaced segments. At 80 keV a gauge volume down to $20 \times 20 \times 270\ \mu m^3$ was selected by the crossed-beam technique.

Typical results are shown in Fig. 9. The variation in radial strain along a given diameter was small, of the order of $\pm 3 \times 10^{-4}$. The axial lattice strains, however, showed a very strong variation with radial position showing a strong shift toward compression near the fiber interface. The strain variation was independent of axial position even when measurements were made far from the end of the fibers. A "knee" in the axial lattice strains at midradius was observed. This is related to strong variations in texture (measured simultaneously). The observed strain variations are not consistent with standard theory based on the strains being related to thermal expansion, plastic or elastic mismatch between the W fiber and Cu matrix. Instead we propose that the observed compressive shifts are caused by the deformation of the Cu matrix by the W-fiber segments as they slipped relative to the matrix during wire drawing. This would result in a uniaxial compressive stress in the core of the Cu matrix balanced by tensile stresses toward the sample surface, which is a similar process to that of inducing biaxial stresses by grinding.

C. Local Deformation in Stainless Steel

An experimental verification of advanced polycrystal deformation models that are expected to encompass specific grain-to-grain interactions can be provided by examining the statistical distribution of the stress states of individual grains of specific crystallagraphic orientation in prestrained steel samples. Neutron diffraction only provides average values of the stresses and requires large grain sizes if distinct grains should be observed.

Cylindrical stainless-steel specimens with a diameter of 4.5 mm and an average grain size of 30 μm were prestrained to various deformations close to the elastic limit.

Sixty-eight keV x rays were selected from the synchrotron beam by a perfect Si monochromator. A rather large beam size of $0.4 \times 0.4\ mm^2$ was defined by a pinhole, and the longitudinal resolution was not confined. The total number of grains within the illuminated sample volume was still sufficiently small that reflections from individual grains were separated. The samples were mounted on the ω axis of a two-axis diffractometer, and the strain was measured by a perfect Si analyzer crystal mounted on the 2Θ axis. Several local volume elements and Bragg reflections, with the scattering vector along axial and radial direction, were investigated for each sample. For each grain a two-dimensional ω-2Θ mapping was performed. From such maps statistics can be extracted on the strain of the grains (2Θ center positions) and on grain perfection (peak widths in the two directions). A dramatic increase of the peak width in ω direction was observed with increasing degree of plastic deformation.

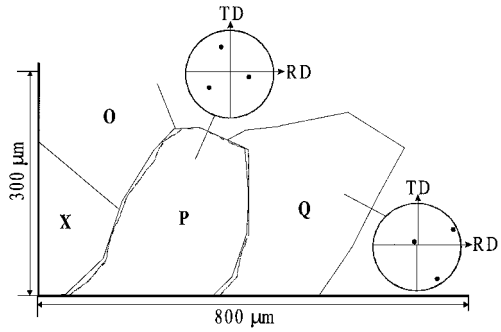

Fig. 10 Part of the grain map showing four grains in the Cu sample. The orientations are indicated by pole figures (RD = rolling direction, TD = transverse direction). The boundaries of the P grain are indicated as obtained from a P grain reflection (——) and from reflections of neighboring grains (– – –).

The combined observation of the variance of the strains (from this study) and the average strains (also from neutron diffraction) of the grains will be compared to poly-crystal deformation theory. Furthermore, we speculate that it may be possible to follow the effect of tensile deformation on gliding and rotation of the individual grains by analyzing the peak broadening as a function of deformation.

D. Characterization of Grain Boundaries in Copper

The grain boundaries of a Cu specimen were mapped and the results compared to those obtained by electron microscopy (EBSP). Therefore the grain orientation and topology at the surface of a Cu bar of 3×3 mm^2 cross section were characterized by EBSP. High-energy synchrotron radiation was then used to investigate the sample in transmission geometry. The layer just below the surface was compared to the EBSP results.

An incident beam of 20×20 μm^2 was selected by a pinhole from the monochromatized, broad energy band, unfocused, synchrotron radiation. The specimen was aligned with the surface to be characterized parallel to the incident beam, and the edges of the sample were determined as reference position with a precision of 10 μm. The longitudinal resolution was obtained by means of a (first generation) conical slit cell and a two-dimensional detector (Fig. 5). The energy was tuned to 88.08 keV to match the opening angles of the conical slit cell. The gap of the conical slit openings of this cell was 50 μm, leading to a $20 \times 20 \times 500$ μm^3 trapezoidal gauge volume. The grains were brought into reflection position by an ω rotation, and the grain boundaries were found by sample translation as defined by points of half intensity.

The grain orientations obtained by the two methods agreed within the EBSP accuracy of about 1 deg; a part of the grain map is shown in Fig. 10. The maximum deviation in grain boundary positions were 25 μm. Consistency checks of the x-ray measurements showed deviations up to 20 μm. Further examples of grain mappings are described in Ref. 11.

V. Conclusions

High-energy synchrotron radiation has proven to be a powerful tool for the local characterization of polycrystalline bulk materials. The technique is nondestructive, and a spatial resolution on the μm level can be achieved. Feasibility experiments demonstrated the potential for in situ local strain scanning and grain boundary topology.

A first, dedicated experimental station has been constructed at the ESRF. The technique has been advanced by the instrumentational developments of focusing optics, conical slit cells, and high-resolution position sensitive detectors. First results of the commissioning indicate that a spatial resolution down to 1 μm in one dimension, and $5 \times 5 \times 50$ μm^3 in three dimensions becomes feasible with substantial photon flux. Most of the encountered limitations are of a technological rather than a fundamental nature. Further progress is therefore expected. However, unique information on the mesoscopic scale is provided already. Substantial effort will be devoted to the development of routine experimental procedures, and the 3DXRD experimental station became accessible for external users in late 1999.

In situ studies are of central interest, and, in addition to the existing simple furnace and combined torsion cell/furnace, a stress rig is available. In combination with the described methods for parallel data acquisition, truly three-dimensional mappings should become possible on reasonable timescales. Software must be developed that efficiently handles the high data rates produced by the two-dimensional detectors.

Finally, it would be natural to combine microdiffraction with high-resolution high-energy imaging, as a close analog to the combined use of the scanning and diffraction modes in the electron microscope. The obtained microfocus might be used as a radiation source for projection imaging. So far, however, no experimental tests have been performed.

Acknowledgments

The authors are indebted to many scientists and technicians of the Risø Materials Research Department and the ESRF Experiments Division for their devoted contributions. Support for this work was provided by DanSync and STVF.

References

[1] Allen, A. J., Hutchings, M. T., Windsor, C. G., and Andreani, C., "Neutron Diffraction Methods for the Study of Residual Stress Fields," *Advances in Physics*, Vol. 34, No. 4, 1985, pp. 445–473.

[2] Kvick, Å., and Poulsen, H. F., "Local Characterisation of Materials by Synchrotron Radiation," Workshop Proceedings, Internal ESRF Publ. ESRF97KV10T, Grenoble, France, Feb. 1997.

[3] Poulsen, H. F., Garbe, S., Lorentzen, T., Juul Jensen, D., Poulsen, F. W., Andersen, N. H., Frello, T., Feidenhans'l, R., and Graafsma, H., "Applications of High-Energy Synchrotron Radiation for Structural Studies of Polycrystalline Materials," *Journal of Synchrotron Radiation*, Vol. 4, 1997, pp. 147–155.

[4] Lauridsen, E. M., Juul Jensen, D., Poulsen, H. F., and Lienert, U., "Kinetics of Individual Grains During Recrystallization," *Scripta Mettalurgica* (to be published).

[5] Lorentzen, T., "Numerical Analysis of Instrumental Resolution Effects on Strain Measurements by Diffraction near Surfaces and Interfaces," *Journal of Neutron Research*, Vol. 5, No. 3, 1997, pp. 167–180.

[6] Webster, P. J., Mills, G., Wang, X. D., Kang, W. P., and Holden, T. M., "Impediments to Efficient Through-Surface Strain Scanning," *Journal of Neutron Research*, Vol. 3, No. 4, 1996, pp. 223–240.

[7] Lienert, U., Schulze, C., Honkimäki, V., Tschentscher, T., Garbe, S., Hignette, O., Horsewell, A., Lingham, M., Poulsen, H. F., Thomsen, N. B., and Ziegler, E., "Focusing Optics for High Energy Diffraction," *Journal of Synchrotron Radiation*, Vol. 5, 1998, pp. 226–231.

[8] Schulze, C., Lienert, U., Hanfland, M., Lorenzen, M., and Zontone, F., "Microfocussing of Hard X-Rays with Cylindrically Bent Crystal Monochromators," *Journal of Synchrotron Radiation*, Vol. 5, 1998, pp. 77–81.

[9] Underwood, J. H., Thompson, A. C., Wu, Y., and Giauque, R. D., "X-ray Microprobe Using Multilayer Mirrors," *Nuclear Instruments and Methods in Physics Research A*, Vol. 266, 1988, pp. 296–302.

[10] Nielsen, S. F., Wolf, A., Poulsen, H. F., Ohler, M., Lienert, U., and Owen, R. A., "A Conical Slit for Three-Dimensional XRD Mapping," *Journal of Synchrotron Radiation*, Vol. 7, 2000, pp. 103–109.

[11] Juul Jensen, D., Kvick, Å., Lauridsen, E. M., Lienert, U., Margulies, L., Nielsen, S. F., and Poulsen, H. F., "Plastic Deformation and Recrystallization Studied by the 3D X-Ray Microscope," *Materials Research Society Symposium Proceedings*, Vol. 590, Materials Research Society, 2000, pp. 227–240.

[12] Lienert, U., Poulsen, H. F., Honkimäki, V., Schulze, C., and Hignette, O., "X-Ray Optics for the Local Structural Characterization of Materials with Synchrotron Radiation," *Journal of Synchrotron Radiation*, Vol. 6, 1999, pp. 979–984.

[13] Lienert, U., Poulsen, H. F., Martins, R. V., and Kvick, Å., "A High Energy Microscope for Local Strain Measurements Within Bulk Materials," *Materials Science Forum*, Vol. 347–349, 2000, pp. 95–100.

[14] Lienert, U., Martins, R., Grigull, S., Pinkerton, M., Poulsen, H. F., and Kvick, Å., "High Spatial Resolution Strain Measurements Within Bulk Materials by Slit-Imaging," *Materials Research Society Symposium Proceedings*, Vol. 590, Materials Research Society, 2000.

[15] Lorentzen, T., Clarke, A. P., Poulsen, H. F., and Garbe, S., "Local Strain Contours Around Inclusions in Wire-Drawn Cu/W Composites," *Composites Part A*, Vol. 28, No. 7, 1997, pp. 667–674.

A. M. Waas
Associate Editor